High temperature gradient micro-sensor for wall shear stress and flow direction measurements

Cécile Ghouila-Houri, J. Claudel, J.C. Gerbedoen, Q. Gallas, E. Garnier, A. Merlen, R. Viard, Abdelkrim Talbi, Philippe Pernod

Applied Physics Letters

High temperature gradient micro-sensor for wall shear stress and flow direction measurements

Cite as: Appl. Phys. Lett. **109**, 241905 (2016); https://doi.org/10.1063/1.4972402
Submitted: 26 October 2016 • Accepted: 03 December 2016 • Published Online: 16 December 2016

C. Ghouila-Houri, J. Claudel, J.-C. Gerbedoen, et al.

High temperature gradient micro-sensor for wall shear stress and flow direction measurements

C. Ghouila-Houri,[1,2,a)] J. Claudel,[1] J.-C. Gerbedoen,[1] Q. Gallas,[2] E. Garnier,[2] A. Merlen,[1,2] R. Viard,[3] A. Talbi,[1] and P. Pernod[1]
[1]*Univ. Lille, CNRS, Centrale Lille, ISEN, Univ. Valenciennes, UMR 8520 - IEMN/LIA LICS, F-59000 Lille, France*
[2]*ONERA, Chemin de la Hunière, 91123 Palaiseau, France*
[3]*Fluiditech, Thurmelec, 68840 Pulversheim, France*

(Received 26 October 2016; accepted 3 December 2016; published online 16 December 2016)

We present an efficient and high-sensitive thermal micro-sensor for near wall flow parameters measurements. By combining substrate-free wire structure and mechanical support using silicon oxide micro-bridges, the sensor achieves a high temperature gradient, with wires reaching 1 mm long for only 3 μm wide over a 20 μm deep cavity. Elaborated to reach a compromise solution between conventional hot-films and hot-wire sensors, the sensor presents a high sensitivity to the wall shear stress and to the flow direction. The sensor can be mounted flush to the wall for research studies such as turbulence and near wall shear flow analysis, and for technical applications, such as flow control and separation detection. The fabrication process is CMOS-compatible and allows on-chip integration. The present letter describes the sensor elaboration, design, and micro-fabrication, then the electrical and thermal characterizations, and finally the calibration experiments in a turbulent boundary layer wind tunnel. *Published by AIP Publishing.*
[http://dx.doi.org/10.1063/1.4972402]

Accurate near wall flow measurements play a key role for many technical applications[1] such as flow control in domains including aerospace and aeronautics, micro-fluidics, process control, lab-on-chip, or micro-mechanical valve development[2] and for the study of unsteady flows and turbulence. When measuring fluctuation quantities in high Reynolds number turbulent boundary layers, flow sensors have to resolve both small length- and velocity-scales at high frequencies, in the view of Kolmogorov scales.[3] Therefore, very small, fast, and high sensitive measurement devices are needed and Micro-Electro-Mechanical Systems (MEMS) technology allows the development of miniaturized flow sensors that can fulfill such requirements in terms of high spatial and temporal resolution performances as well as low-cost mass production and high reliability.

Micro-machined flow sensors can be classified into two groups based on different measurement methods: "direct" or "indirect" measurement sensors.[4] The first ones usually use a floating element displaced laterally by tangential viscous forces in the flow. The movement implies a variation of an electrical parameter: capacitive sensors[5] or cantilever based sensors[6,7] are part of this category. For indirect flow measurement, various methods have been applied as, for example, micro-fences using a cantilever structure and piezoresistors,[8] optical resonance such as whispering gallery modes of dielectric microspheres shifting with radial deformations of the spheres due to the shear stress,[9] the deflection of micro-pillars,[10] and thermal-based sensors,[11–20] which are developed below. Among all these devices, thermal sensors are widely adopted when dealing with fluid dynamics, including laminar or turbulent flows, as they do not contain mechanical moving parts and are thus less prone to wear than the others.

Thermal flow sensors are themselves classified into two categories: hot-wire sensors and hot-film sensors. The difference between them lies in the designed structure: in hot-wire sensors the metallic wire resistor is free from the substrate and placed within the flow, whereas in hot-film sensors it is deposited on a membrane placed adjacent to the flow. Hot-film sensors suffer from heat losses in the membrane on which the metallic wire is deposited: various materials have thus been used such as silicon nitride,[11,12] glass,[13] or flexible polymer.[14,15] These sensors are nonetheless often used for flow separation detection and wall shear stress measurement as they are robust and easy to mount flush to the wall. Hot-wire sensors are mainly free from the substrate, which enables an optimal heating uniformity and high sensitivity,[16–19] but they are more fragile than hot-film sensors.

In this letter, we present a thermal sensor designed for flow control applications and separation detection, whose structure is a compromise between conventional hot-wire and hot-film sensors.[21] In our case, the heating and measurement elements consist in very high aspect ratio metallic wires free from the substrate and suspended using periodic silicon oxide micro-bridges. This design allows an efficient thermal insulation as well as a mechanical robustness. The sensor operates in a constant current anemometric mode or a constant temperature anemometric mode and is sensitive to the near wall flow fluctuating parameters: wall shear stress and flow direction.

The device geometry (Fig. 1(a)) consists in four 1-mm-long and 3-μm-wide wires, free from the substrate but supported by silicon oxide micro-bridges over a 20-μm-deep cavity. One wire is the heater and the other three are measurement wires. The heater is over a measurement wire: they form a multilayer at the center of the sensitive part with a layer of silicon oxide ensuring electrical insulation between them. Measure and heating are indeed electrically uncoupled to

[a)]Electronic mail: cecile.ghouila@onera.fr

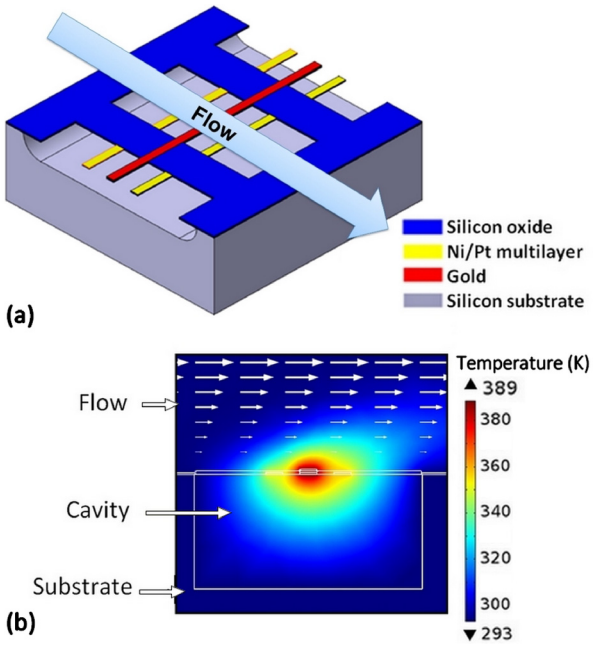

FIG. 1. (a) Schematic of the proposed sensor design. (b) Working principle simulated on COMSOL multiphysics.

improve the signal to noise ratio. The other measurement wires are arranged on both sides of this central element. Each wire is separated from the substrate to avoid heat losses by solid conduction into the substrate and to increase gaseous conduction. The sensitive elements exhibit a very high aspect ratio (length versus width) of 333 to perform high sensitivity enhanced by proper temperature uniformity and high temperature gradient. The oxide silicon micro-bridges provide the structure mechanical toughness over the fluid flow despite the wires' length. The mechanical stress in this design is engineered using multilayer materials enabling a self-compensating stress. Measurement wires are indeed 20 nm-Ni/30 nm-Pt multilayers reaching a total thickness of 120 nm.

When the gold resistor is heated by an electric current, the heat is transferred to the measurement wires and the surrounding fluid by conduction (Fig. 1(b)). The changes in heat distribution on the wires imply a temperature change at the wires' level. Temperature variations cause the material resistivity to change and consequently imply resistance variations in the measurement wires. Here, we chose a Ni/Pt multilayer as it allows high resistance sensitivity to temperature as described when dealing with electro-thermal characterizations.

Figure 2 shows the micro-machining process performed on a 3-in. (100) silicon wafer allowing the manufacture of about 140 sensors.

First, 300 nm of silicon oxide (SiO_2) was deposited using Plasma Enhanced Chemical Vapor Deposition (PECVD). Measurement wires were then patterned using photo-lithography techniques, and the Ni/Pt multi-layer was deposited by evaporation. The metal was then removed using lift-off techniques to precisely define the wires. Another layer of SiO_2 was deposited using Low Pressure Chemical Vapor Deposition (LPCVD). The heater was then patterned using the same techniques as for the wires: photo-lithography, metalization by evaporation, and lift-off. The next step was to etch the micro-bridges using the Reactive Ion Etching (RIE) technique

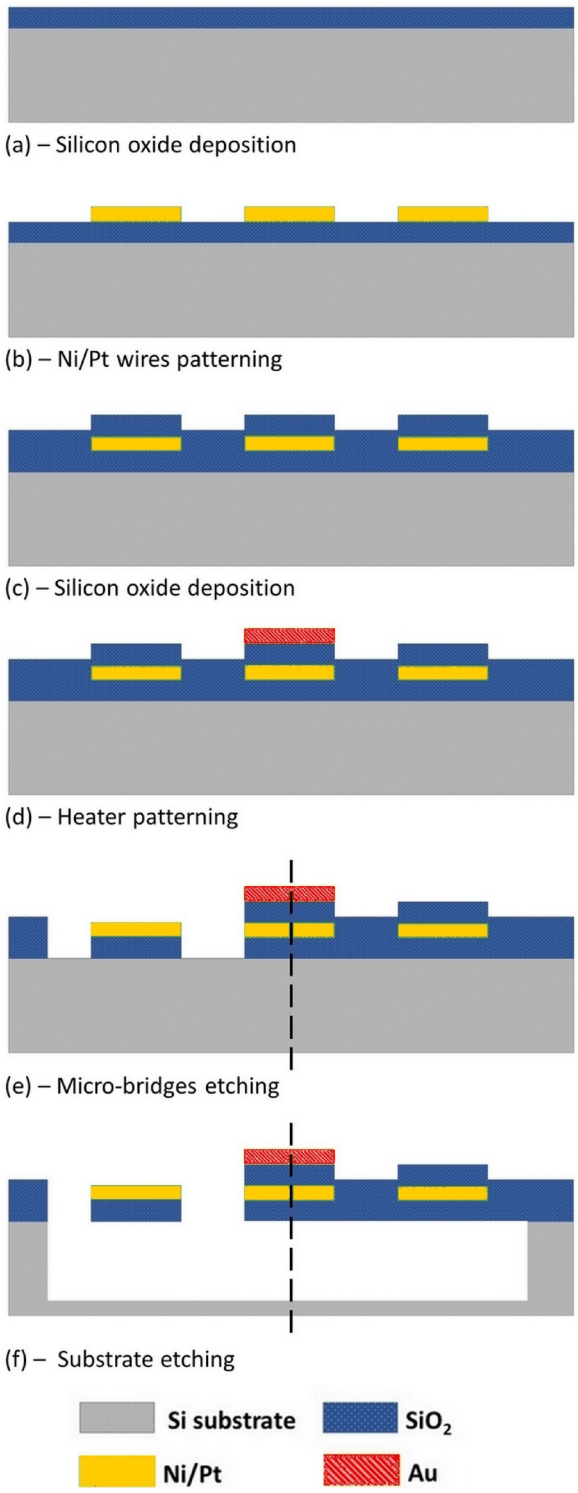

FIG. 2. Micro-machining process.

with CF_4/ChF_3 plasma gas. On the corresponding picture (e) from Figure 2, two different sections are shown: the left one is the cross-section where there is no bridge and the right one is the section of the silicon oxide bridge. After etching the micro-bridges, large gold pads, for contact recovering, were defined and patterned (this step is not shown in Figure 2). The wafer was then cut to separate all the sensors. Finally, each sensor was etched using the XeF_2 plasma to separate the wires and the bridges from the substrate (Fig. 2(f)) by isotropic etching.

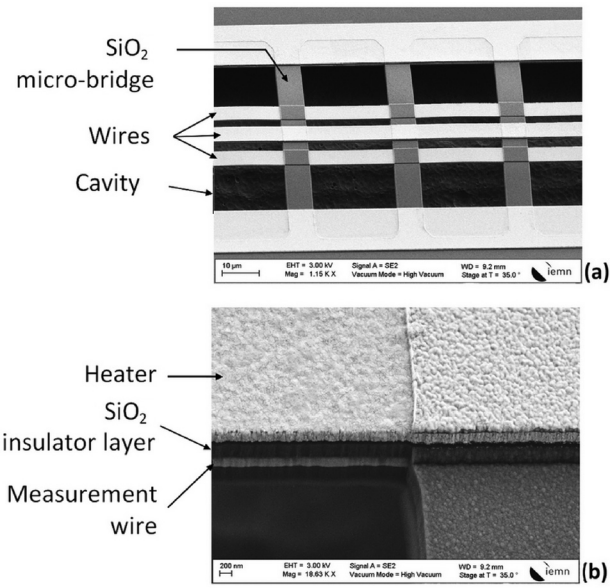

FIG. 3. (a) SEM picture of the manufactured hot-wire sensor. (b) Zoom on the central wire.

Figures 3(a) and 3(b) are Scanning Electron Microscopy (SEM) pictures of our manufactured micro-sensor: Figure 3(a) shows the complete structure with the micro-bridges supporting the wires and Figure 3(b) is a zoom on the central elements, allowing us to distinguish the heater (upper layer) from the measurement wire (lower layer).

Next, we experimented both electrical and thermal characterizations of the sensor, without fluid flow. First, we experimentally determined the Temperature Coefficient of Resistance (TCR) provided by the Ni/Pt multilayer. The TCR is a material characteristic, defined by $TCR = \Delta R/(\Delta T \cdot R_0)$, where R_0 is the resistance of reference at 25 °C, ΔR is the resistance variation, and ΔT is the temperature variation. We used a hot plate and a probe station for the measurements. The resistance variations with temperature exhibit a linear behavior between 20 °C and 70 °C resulting in a TCR of about 2380 ± 70 ppm/°C, with TCR dispersion measured across the 3-in. diameter wafer. Afterwards, the electrical temperature rise coefficient was measured. It represents the heating ability of the wires when the heater is crossed by an electric current ranging from 0 to 7 mA and then provides the information on the thermal insulation quality. The measurement set up uses a Keithley 2400 sourcemeter and a probe station. Experimentally, the temperature rise coefficient reaches 7.8 ± 0.9 K/mW for the central measurement wire and 5.0 ± 0.8 K/mW for the lateral wires (Fig. 4).

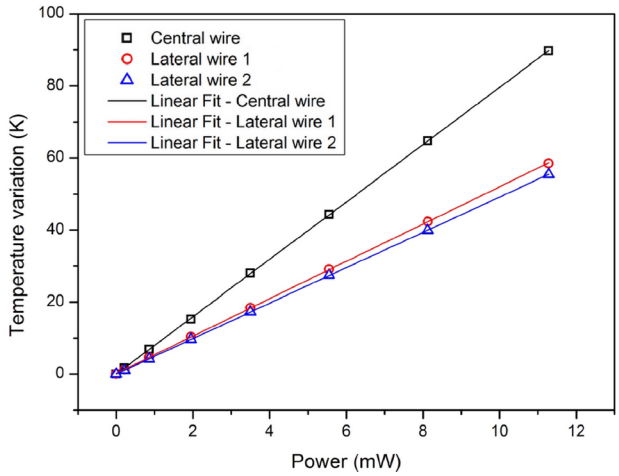

FIG. 4. Electrical characterization of the sensor for both central and lateral wires and comparison with numerical results.

Finally, we characterized the sensor response to the fluid flow in a turbulent boundary layer wind tunnel located at the ONERA Lille center (Fig. 5(a)). This 30 cm × 30 cm test section wind tunnel operates with velocities ranging from 0 m/s to about 40 m/s. The sensor is mounted flush to the wall (Fig. 5(b)). The flow velocity in the wind tunnel is measured by a Dantec hot-wire probe and a proper boundary layer characterization allowed us to deduce the corresponding wall shear stress.

We characterized the sensor by measuring the resistance variations simultaneously with the wall shear stress fluctuations. We performed the experiments using the sensor in the constant current mode, with a heating current of 7 mA, corresponding to about 11 mW. Results (Fig. 6) show the resistance variations ΔR with wall shear stress ($\Delta R = \frac{R(0\,\mathrm{Pa}) - R(x\,\mathrm{Pa})}{R(0\,\mathrm{Pa})}$) for both central and lateral wires. The wires are placed perpendicular to the flow; therefore, the lateral wires are distinguished as upstream and downstream of the flow. As they share electrical and thermal characteristics, the difference of resistance variation present here for more than 0.4 Pa is only due to the flow direction. The wire upstream of the flow is more cooled than the wire downstream.

The flow direction measurements were performed using the resistance difference between the two lateral wires. The general aim is to provide a way to detect the presence of a flow separation since in such a situation, the velocity field near the wall is reversed. The sensor setup in the wind tunnel enables us to rotate it from 0° to 180°. The results are shown in Figure 7 and present the variation of the difference of resistance between the two lateral wires. The reference is taken for 90° when the sensor wires are parallel to the flow,

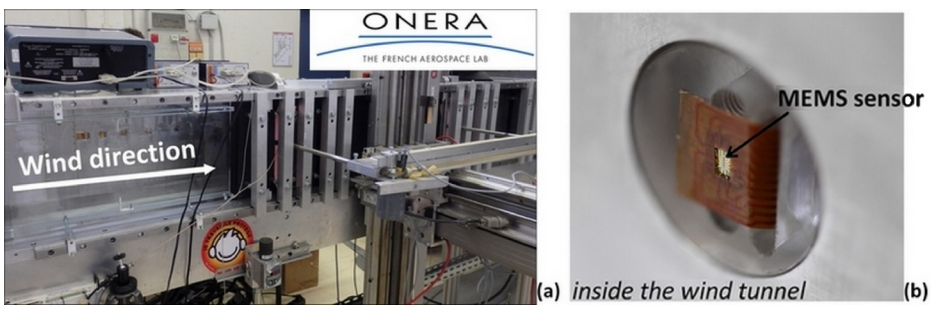

FIG. 5. (a) Turbulent boundary layer wind tunnel in ONERA Lille. (b) MEMS sensor mounted on the wall.

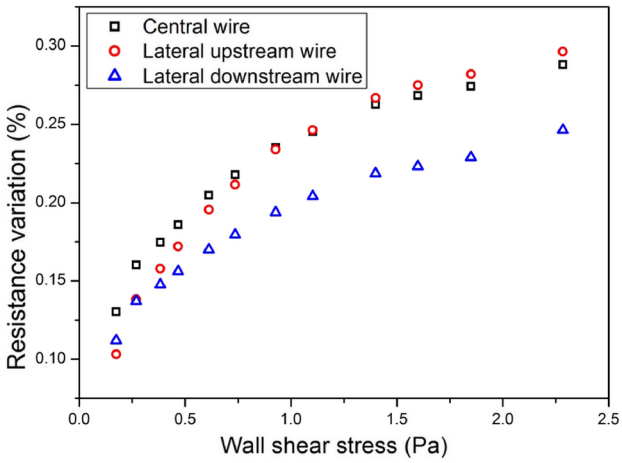

FIG. 6. Resistance variation versus wall shear stress for both central and lateral wires.

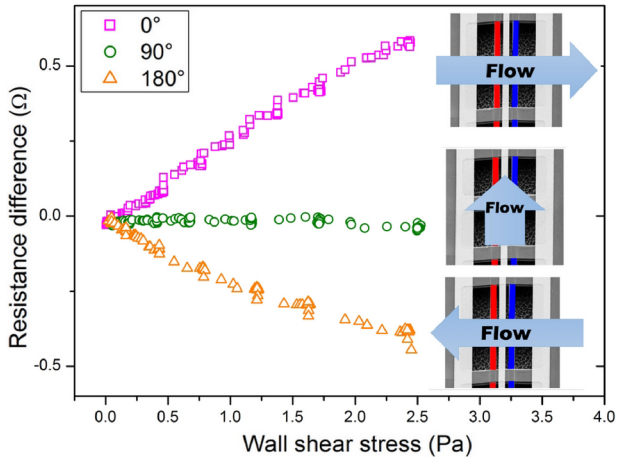

FIG. 7. Resistance variation of the difference of resistance between the two lateral wires versus wall shear stress for different flow directions: 0°, 90°, and 180°.

and thus the lateral resistances are almost equal. At 0° and 180°, the sensor wires are perpendicular to the flow, but at 180° the two lateral wire positions are inversed compared to 0°. The response presents an apparent dissymmetry that is explained by the mounting imperfections of the sensor on the support.

As a conclusion, we elaborated an efficient and high sensitive micro-sensor for near wall flow measurements. We presented the design (free hot-wires supported by silicon oxide micro-bridges), the fabrication process, the electro-thermal characterizations, and the wind tunnel experimental results. The sensor demonstrates a high sensitivity to the near wall flows, with up to 0.3% resistance variation for 2.4 Pa, as well as a low power consumption (11 mW). The fabrication using micro-machining techniques allows low cost and high volume production and the possibility of on-chip integration.

This work was funded by the French National Research Agency (ANR) in the framework of the ANR ASTRID "CAMELOTT" Project. It was supported by the regional platform CONTRAERO in the framework of the CPER ELSAT 2020 Project. The authors also thank RENATECH, the French national nanofabrication network, and FEDER.

[1]L. Lofdahl and M. Gad-el-Hak, Prog. Aerosp. Sci. **35**, 101 (1999).
[2]O. Ducloux, A. Talbi, L. Gimeno, R. Viard, P. Pernod, V. Preobrazhensky, and A. Merlen, Appl. Phys. Lett. **91**, 034101 (2007).
[3]L. Jacquin, Aerosp. Lab J. **1**, AL-01 (2009).
[4]L. Lofdahl and M. Gad-El-Hak, Meas. Sci. Technol. **10**, 665 (1999).
[5]V. Chandrasekharan, J. Sells, J. Meloy, D. P. Arnold, and M. Sheplak, J. Microelectromech. Syst. **20**, 622 (2011).
[6]S. Zhang, L. Lou, and C. Lee, Appl. Phys. Lett. **100**, 023111 (2012).
[7]P. Chen, Y. Zhao, and Y. Li, in 9th IEEE International Conference on NEMS (2014).
[8]T. von Papen, U. Buder, H. D. Ngo, and E. Obermeier, Sens. Actuators A **113**, 151–155 (2004).
[9]U. K. Ayaz, T. Ioppolo, and V. Otugen, AIAA Paper No. 2011–337, 2011.
[10]S. Grosse and W. Schruder, AIAA J. **47**, 314 (2009).
[11]Y. Ou, F. Qu, G. Wang, M. Nie, Z. Li, W. Ou, and C. Xie, Appl. Phys. Lett. **109**, 023512 (2016).
[12]E. Vereshchagina, R. Tiggelaar, R. Sanders, R. Wolters, and J. Gardeniers, Sens. Actuators B **206**, 772 (2015).
[13]Y. Zhu, M. Qin, J. Huang, Z. Yi, and Q.-A. Huang, IEEE Sens. J. **16**, 4300–4308 (2016).
[14]T. Leu, J. Yu, J. Miau, and S. Chen, Exp. Therm. Fluid Sci. **77**, 167 (2016).
[15]J. Miau, T. Leu, J. Yu, J. Tu, C. Wang, V. Lebiga, D. Mironov, A. Pak, V. Zinovyev, and K. Chung, Sens. Actuators A **235**, 1 (2015).
[16]A. Talbi, L. Gimeno, J.-C. Gerbedoen, R. Viard, A. Soltani, V. Mortet, V. Preobrazhensky, A. Merlen, and P. Pernod, J. Micromech. Microeng. **25**, 125029 (2015).
[17]M. Laghrouche, A. Adane, J. Boussey, S. Ameur, D. Meunier, and M. Tahanout, AIP Conf. Proc. **1019**, 531–535 (2008).
[18]Y. Fan, G. Arwartz, T. W. van Burden, D. E. Hoffman, and M. Hultmark, Exp. Fluids **56**, 138 (2015).
[19]A. Persson, V. Lekholm, G. Thornell, and L. Klintberg, Appl. Phys. Lett. **106**, 194103 (2015).
[20]Y. Kessler, S. Krylov, and A. Liberzon, Appl. Phys. Lett. **109**, 083503 (2016).
[21]R. Viard, A. Talbi, A. Merlen, P. Pernod, C. Frankiewicz, and J.-C. Gerbedoen, J. Micromech. Microeng. **23**, 065016 (2013).